Materials Science-Poland, 37(2), 2019, pp. 158-165
http://www.materialsscience.pwr.wroc.pl/
DOI: 10.2478/msp-2019-0019

sciendo

Growth, solvent effect, optical and electrical properties of sodium 4-hydroxybenzenesulfonate dihydrate

ZAHID MD. I.[1], MALARKODI A.[2], MEERA SREENARAYANAN[3], MEERA K.[3], JOSEPH WILSON K.S.[2], MOHAN KUMAR R.[1,*]

[1]Presidency College, Department of Physics, Chennai-600005, India
[2]Arul Anandar College, Department of Physics, Madurai-625514, India
[3]Women's Christian College, Post Graduate Department of Physics, Chennai-600006, India

Single crystal of sodium 4-hydroxybenzenesulfonate dihydrate (Na-4-HBS) was grown from an aqueous solution by slow evaporation method. Powder X-ray diffraction study was carried out to identify the lattice parameters of the crystal. FT-IR spectral analysis confirmed the existence of various functional groups in the compound. The optical transmittance, cut-off wavelength and band gap energy were estimated from the UV-Vis studies. Photoluminescence studies revealed the transition mechanism by optical excitation. The variation of dielectric properties and AC conductivity of the grown crystal with frequency was studied at different temperatures. Measurements of mechanical properties of Na-4-HBS were carried out to find the hardness of the material. The laser induced surface damage threshold and relative second harmonic generation nonlinear optical properties of the grown crystal were studied using Q-switched Nd:YAG laser.

Keywords: *solvents; single crystal growth; nonlinear optical material; electrical properties*

1. Introduction

During the past few decades, intensive research efforts have been made to explore new materials for variety of nonlinear optical (NLO) applications, since these materials play a vital role in the photonic technology, including optical information processing, telecommunication, optical storage, THz generation and detection [1, 2].

In addition to the high optical nonlinearities, these materials should also exhibit favorable physical properties. Here, various steps have been taken to share the properties of both organic and inorganic compounds, by stoichiometric bonding of the polarizable organic molecules with an inorganic host. Alternative and closely related strategy has been adopted to form metal-coordination complexes of highly polarizable organic molecules [3].

Organometallic compound hexakis(thiourea)nickel(II)nitrate was found to be a centrosymmetric crystal with significant SHG efficiency [4]. Liquid crystalline behavior of sodium dodecyl benzenesulfonate has been studied based on its physical parameters such as ultrasonic velocity, density and viscosity [5]. Sodium sulfanilate dihydrate crystals were grown to study their NLO applications [6]. Sodium p-nitrophenolate dihydrate has proven its usefulness as a semi-organic nonlinear optical material [7]. The crystal structure of 4-methylanilinium 4-hydroxybenzenesulfonate was solved and reported to have nonlinear optical properties [8]. Taffarel et al. [9] investigated adsorption of sodium dodecyl benzenesulfonate from aqueous solution using modified natural zeolite with cetyltrimethylammonium bromide. Glycine picrate, a centrosymmetric crystal showed remarkable second harmonic generation properties [10]. Zirconium phenylphosphonate, $Zr(C_6H_5PO_3)_2$, a novel metal phosphonate material, was reported [11] and its physical properties have been controlled by using different organic groups. Based on this report, we focused our interest on synthesizing and characterizing sodium 4-hydroxybenzenesulfonate dihydrate

*E-mail: mohan66@hotmail.com

$Na_2(HOC_6H_2SO_3)_2{\cdot}4H_2O$) prepared from sodium carbonate and p-hydroxybenzenesulfonic acid. The compound contains alternating layers of sulfonate ions and hydrated cations. In its structure, sodium ions coordinate directly to the sulfonate oxygen atoms. The presence of hydroxyl groups on the phenyl rings allows an enhanced hydrogen bonding between the layers [12]. In the present study, bulk crystal of Na-4-HBS was grown from aqueous solution and the structural, optical, laser induced surface damage threshold, SHG, electrical and mechanical properties have been studied.

2. Experimental

2.1. Synthesis and solvent effect on the growth mechanism

Na-4-HBS compound was synthesized from commercially available sodium carbonate (Sigma Aldrich, 99 %) and 4-hydroxybenzenesulfonic acid (Sigma-Aldrich, 40 %). The starting materials were dissolved in deionized water in 1:2 ratio. The solution was stirred for 4 h and after attaining saturation, it was filtered and kept in a clean environment. After four days, crystals were obtained by using slow evaporation technique. Since the solubility of the material plays a vital role in yielding good shaped crystals, it is desired to select a suitable solvent for the material, where the solute is moderately soluble. The solubility of Na-4-HBS in polar solvents like water, methanol, ethanol and acetone was measured at room temperature to probe the solvent effect on the growth habit of the crystal. Initially, Na-4-HBS salt was made to dissolve in ultra-pure deionized water (Millipore, resistivity 18 MΩ), methanol (Sigma-Aldrich, 99.8 %), ethanol (Merck, 98.9 %), and acetone (Merck, 99.8 %), respectively. It was observed that Na-4-HBS is soluble in all the four solvents, but the growth rate and growth habits are different in different solvents. In case of deionized water, the growth rate was low in b-axis while in case of other solvents the growth rate was much faster in b-axis even though an effort has been taken to control evaporation. It is noticed from Fig. 1 that the crystal yielded from the water solvent has good growth habit and is highly transparent with growth rate along all the directions, while the crystals yielded from other solvents have a needle shape and thin plates. In the present study, the crystal grown from the water solvent has been subjected to various characterizations. The solubility, crystal habit and growth period of Na-4-HBS crystal in various solvents are summarized in Table 1.

2.2. Solubility and crystal growth

The solubility of Na-4-HBS in water was determined as a function of temperature varying from 30 to 60 °C. After attaining saturation, the equilibrium concentration of the solute was analyzed gravimetrically. The corresponding solubility curve is depicted in Fig. 1.

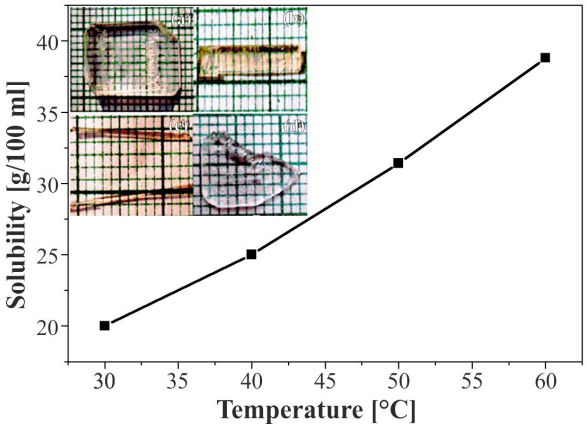

Fig. 1. Solubility of Na-4-HBS at different temperatures using water as solvent; inset: photograph of as-grown Na-4-HBS crystal from (a) water (b) methanol (c) ethanol (d) acetone solvents at pH 4.0.

It shows that the solubility increases significantly with increasing temperature favoring bulk growth of the crystals. Single crystal of Na-4-HBS was grown from aqueous solution by using solvent evaporation technique. Based on the solubility data, 20.32 g of sodium 4-hydroxybenzenesulfonate dihydrate salt was dissolved in 100 mL of deionized water at room temperature and the solution was continuously stirred for 6 h to get a homogeneous solution. The solution was filtered using high quality Whatman filter paper to remove impurities present in the solution, then it was allowed

Table 1. Effect of solvent on the growth mechanism of Na-4-HBS.

Solvents	Solubility [g/10 mL]	Crystal habit	Optical quality	Growth period	Dimension
Water	2.03	Rectangular	Highly transparent	More than a week	15 mm × 20 mm × 4 mm
Methanol	0.82	Needle shaped	Transparent	3 to 4 days	13 mm × 2 mm × 1 mm
Ethanol	0.80	Needle shaped	Transparent	3 days	13 mm × 0.8 mm × 0.3 mm
Acetone	0.65	Thin plates	Transparent	2 days	9 mm × 8 mm × 0.1 mm

for slow evaporation by covering with a perforated sheet. The saturated solution was kept in a clean atmosphere to avoid any impurities. The synthesized compound was recrystallized for three times to improve its purity. The saturated growth solution was prepared using the recrystallized salt, filtered and allowed for slow evaporation at a temperature of 35 °C using a constant temperature bath. After the period of 1 to 2 weeks, optical quality Na-4-HBS crystal of a size up to 15 mm × 20 mm × 4 mm was harvested as shown in Fig. 1a (inset).

3. Results and discussion

3.1. X-ray diffraction analysis

The single crystal X-ray diffraction data was collected by using Bruker Kappa APEX II single crystal X-ray diffractometer. It indicates that the grown crystal belongs to a monoclinic crystal system with $P2_{1/a}$ space group. The estimated cell dimension are a = 8.02 Å, b = 10.11 Å, c = 23.14 Å, β = 94.02°, and V = 1870 Å^3 and the cell parameters are in good conformity with the reported data.

The grown Na-4-HBS crystal was crushed and grinded into uniform fine powder and subjected to powder X-ray diffraction studies using Bruker D8 X-ray diffractometer with CuKα radiation (λ = 1.542 Å). The (h k l) values were determined using the inbuilt HighScore plus program and the lattice parameters of Na-4-HBS were found. The powder XRD peaks were indexed as shown in Fig. 2.

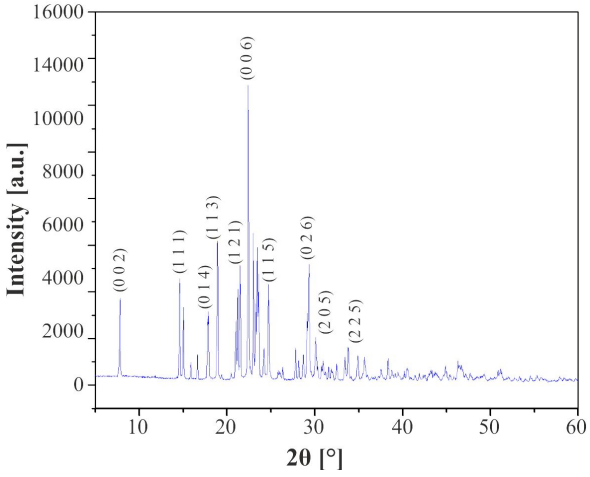

Fig. 2. Powder XRD pattern of Na-4-HBS crystal.

3.2. FT-IR spectral analysis

The sodium 4-hydroxybenzenesulfonate dihydrate crystal was powdered and FT-IR spectrum was recorded to identify the presence of functional groups in the compound. Fourier transform infrared spectrum (400 cm^{-1} to 4000 cm^{-1}) was traced by using BRUKER IFS66VFT-IR spectrometer and the recorded spectrum is shown in Fig. 3. The peak appearing at 3533 cm^{-1} confirms the presence of O–H stretching. The vibrational bands of aromatic C–C stretching in-ring are observed at 1594 cm^{-1} and 1434 cm^{-1}. The vibrations appearing at 1225 cm^{-1} and 1120 cm^{-1} in FT-IR are assigned to C–O stretching and the bending vibration of =C–H is observed at 1032 cm^{-1}.

The –C=C stretching is observed at 1655 cm^{-1}, while =C–H stretching is observed at 3180 cm^{-1}. Two bands corresponding to C=C benzene ring stretching appeared in the range of 1450 cm^{-1} to 1600 cm^{-1}, C–S stretching is observed between

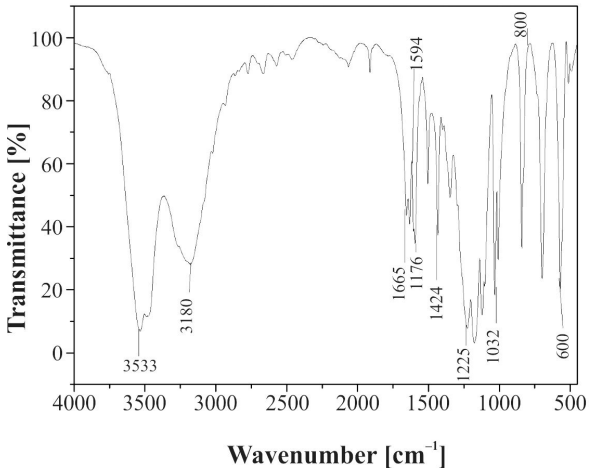

Fig. 3. Infrared spectrum of Na-4-HBS.

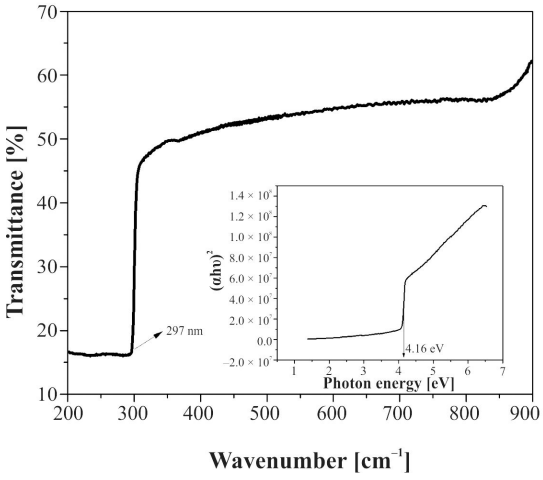

Fig. 4. UV-Vis transmission spectrum; inset: bandgap estimation for Na-4-HBS crystal.

600 cm^{-1} to 800 cm^{-1}, SO_3 stretching is observed at 1176 cm^{-1} [13–15]. From the recorded FT-IR spectra, all prominent functional groups in the compound were identified and the vibrational frequency assignments were given in Table 2.

Table 2. FT-IR vibrational assignments of Na-4-HBS.

υ FT-IR [cm^{-1}]	Assignments
3533	O–H stretch, H–bonded
3180	=C–H stretching
1032	=C-E bending
1594, 1434	aromatic C–C stretching in-ring
1225, 1120	C–O stretching
1655	C=C stretching
600-800	C–S stretching
1176	SO_3 stretching

3.3. Optical studies

3.3.1. UV-Vis NIR transmission studies

UV-Vis studies are helpful in the investigation of NLO materials to find NLO response and spectroscopic absorbance in an appropriate wavelength range. UV-Vis T90+ model spectrometer was used to record the transmission spectra in the wavelength range of 190 nm to 900 nm (Fig. 4).

The grown crystal was cut and polished to a thickness of about 1 mm and it was found that the samples were free from any noticeable defects. From the UV-Vis spectrum, it is evident that the cut-off wavelength of the grown crystal is of 297 nm and the crystal has sufficient transmission window in the entire visible and IR regions which enables good optical transmission for the second harmonic frequency. It means that the grown crystal has an added advantage for optical and optoelectronic device applications. For optical device fabrication, the crystal should have high transparency in a considerable range of wavelength [16–18]. UV-Vis cut-off wavelength of the grown Na-4-HBS crystal was found to be 297 nm. The optical absorption coefficient α was calculated using the relation:

$$\alpha = (1/d)\log(1/T) \tag{1}$$

where d is the thickness of the crystal and T is the transmittance. Owing to the direct band gap, the crystal under study has an absorption coefficient α obeying the following relation for high photon energies hυ:

$$h\upsilon = A(h\upsilon - E_g) \tag{2}$$

where A is a constant, E_g is the optical band gap, h is the Planck constant, and υ is the frequency of the incident photon [19]. The band gap of the grown Na-4-HBS crystal was estimated by plotting $(\alpha h\upsilon)^2$ versus hυ and it is shown in Fig. 4

(inset). The band gap energy of the grown Na-4-HBS crystal was found to be 4.16 eV which makes this material a potential candidate for optical device fabrication.

3.3.2. Photoluminescence spectral analysis

Photoluminescence (PL) spectroscopy is a non-destructive method for probing the optical behavior and electronic structure of materials [20]. The strength of the electron-phonon interaction could be ascribed to the difference between the excitation and emission maximum. PL spectrum was recorded using RF-5301 spectrometer and an inclusion free sample was excited at 308 nm, slightly beyond the UV absorption spectrum level. An intense emission band has appeared in the range of 320 nm to 400 nm, owing to the emission of ultraviolet radiation. PL spectrum of the grown crystal sample (Fig. 5) shows an emission peak at 341 nm (3.6 eV). The emission wavelength is near UV region (320 nm to 400 nm).

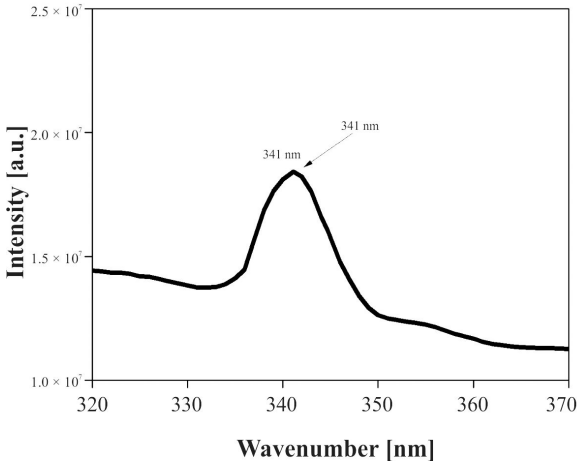

Fig. 5. Photoluminescence spectrum of Na-4- HBS.

Hence, the grown Na-4-HBS crystal shows its potentiality in optical filters and optoelectronic device application [21].

3.4. Dielectric studies

Dielectric properties are correlated with electro-optical properties of crystals. The dielectric study of Na-4-HBS crystal was carried out using HIOKI 3532 LCR TESTER instrument in the frequency region of 50 Hz to 5 MHz. The capacitance of the parallel plate capacitor with the grown crystal sample as a dielectric medium was measured at different frequencies and temperatures.

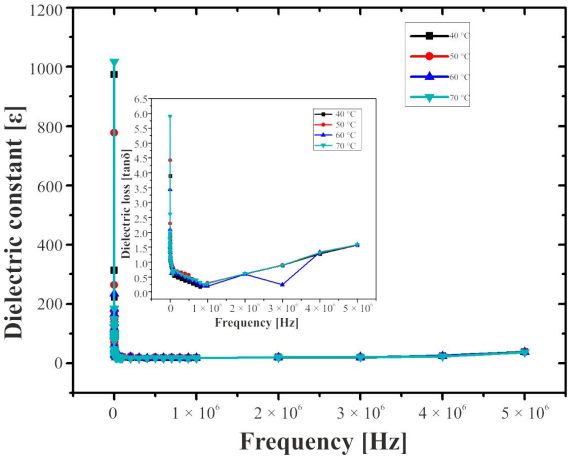

Fig. 6. Variation of dielectric constant; inset: dielectric loss with frequency of Na-4-HBS crystal.

Fig. 6 shows the variation of the dielectric constant and dielectric loss of Na-4-HBS for different frequencies and different temperatures. From the figures, it is observed that the dielectric constant and dielectric loss decrease with increasing frequency and attain saturation at higher frequencies. The low dielectric constant value of the crystal at high frequency is attributed to space charge polarization near the grain boundary interfaces which depends on the purity and perfection of the crystal. The very high value of dielectric constant at low frequencies is due to ionic, electronic, orientation and space charge polarizations. At low frequencies, all the four contributions are active [22]. For a material to be a potential candidate for nonlinear optical applications, dielectric loss tanδ must also be kept as low as possible. From the figure, it is clear that the Na-4-HBS crystal exhibits a very low dielectric loss at high frequencies and it can be used for nonlinear optics applications effectively.

3.5. AC conductivity

AC conductivity study was carried out to characterize the bulk resistance of the crystalline solids. The crystal was subjected to an external electric

field so that redistribution of charges occurred and then a current was induced. The AC conductivity of the sample was calculated using the relation:

$$\sigma_{ac} = \varepsilon_0 \varepsilon_\omega \tan\delta \tag{3}$$

where, ω is the angular frequency. The variation of AC conductivity of Na-4-HBS crystal with frequency is shown in Fig. 7.

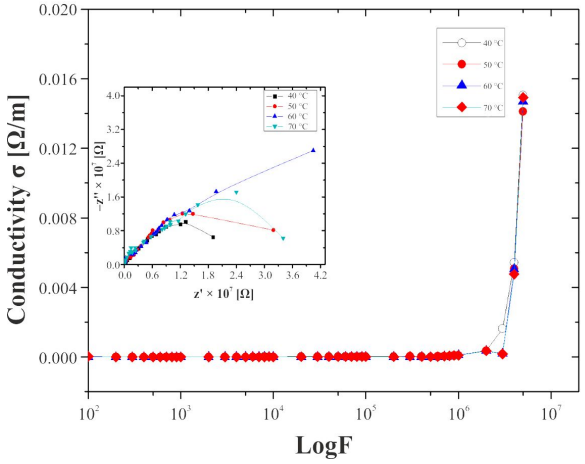

Fig. 7. Variation of AC conductivity with frequency; inset: Nyquist plot drawn between Z' and $-Z''$ of Na-4-HBS crystal.

The conductivity is almost zero at very high frequencies and then it increases with an increase in frequency. At higher frequency, the AC conductivity has increased sharply. The electrical conductivity is proportional to mobility and carrier concentration through the well-known relation: $\sigma = n_d \cdot e \cdot \mu_e$, where e is the electron charge, μ_e is the mobility of electrons and n_d is the number density of electrons. Normally, impedance measurements are made over a range of temperatures and frequencies and analyzed in the complex impedance plane. In AC measurement, the resistance R is replaced by the impedance Z which consists of two parts, $Z = Z' + Z''$. Here, Z is a phasor quantity; a rotating vector may be plotted in rectangular polar, exponential or trigonometric coordinate systems. In the rectangular system, the value of the real part of Z is $Z' = |Z| \cos\theta$ and imaginary part of Z is $Z'' = |Z| \sin\theta$. From these measurements, real and imaginary impedances were evaluated as a function of frequency. Fig. 7 (inset) shows the Nyquist plot between Z' and Z'' of the Na-4-HBS crystal at different temperatures, 40 °C, 50 °C, 60 °C and 70 °C. The arcs can be interpreted by an equivalent circuit model of a nature of a graph which depicts the quality of the capacitor medium. The partial semicircular arc depicts the bulk effect of Na-4-HBS single crystal, since there are no more semicircles. The bulk effect arises due to the parallel combination of bulk resistance and bulk capacitance of the crystal sample.

3.6. Mechanical studies

Hardness of a material is also one of the most important properties, especially for post growth processes and device fabrication. The important property of semi-organic crystals over their organic counterparts is their high mechanical hardness. Indentations were made on a flat, polished surface of the crystal at room temperature for different loads 10 g, 25 g, 50 g and 100 g using Vicker hardness tester fitted with a diamond intender and a light microscope. The Vicker microhardness number H_v was calculated using the relation:

$$H_v = 1.8544 P/d^2 \ \ (\mathrm{kg/mm^2}) \tag{4}$$

where P is the applied load in g, d is the diagonal length of the indentation impression in mm and H_v is the hardness number in kg/mm^2. Fig. 8 illustrates that the Vicker hardness number varies with the applied load and it clearly indicates that the crystal has good mechanical strength.

It is very clear from the figure that H_v increases with an increase of load. When the applied load increases, a few surface layers are penetrated initially and then, with an increase in load, the inner surface layers are penetrated by the indenter. The measured hardness is characteristic of these layers and the increase in hardness number is due to the overall effect on the surface and inner layers of the sample (reverse size indentation effect). Significant cracks occurring around the indentation mark may be due to the release of internal stress generated locally by indentation. The calculated Meyer index number relates the load and indentation diagonal length. The Meyer index n value is used

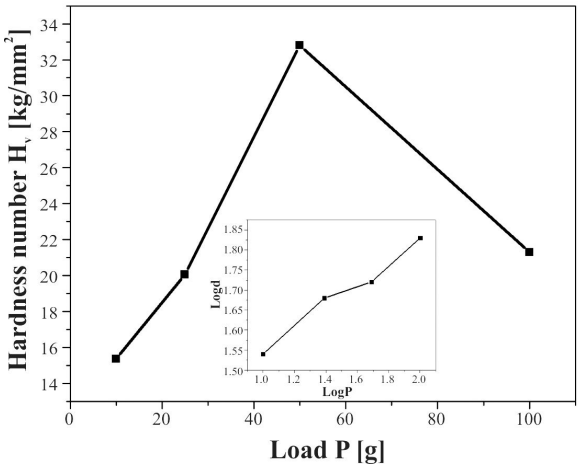

Fig. 8. Variation of hardness number with applied load; inset: a plot of log d vs. log P for Na-4-HBS crystal.

to identify whether the material belongs to soft category or hard category:

$$P = kd^n \tag{5}$$

$$\log P = \log k + n \log d \tag{6}$$

where k is the standard hardness constant for the material and n is the work hardening coefficient. A plot of log d vs. log P is drawn in the inset of Fig. 8 and it is in good agreement with Meyer law. According to Onitsch, the value of n is below 1.6 for hard materials and n $>$ 1.6 for soft materials. The value of n obtained from the slope of the graph was found to be 2.11. Hence, it is concluded that the grown Na-4-HBS crystal belongs to soft material category.

3.7. Second harmonic generation test

The second harmonic generation efficiency of Na-4-HBS crystal was measured by Kurtz-Perry powder technique with potassium dihydrogen phosphate (KDP) crystal as a reference material. The fundamental laser beam of 1064 nm wavelength with 8 ns pulse width and 10 Hz pulse rate, was made to fall normally on the sample cell. The input laser energy incident on the powdered sample was chosen to be 5.65 mJ per pulse. The grown single crystal of Na-4-HBS and reference KDP were ground to a uniform particle size of 125 m to 150 m, packed in a microcapillary of uniform bore size, and exposed to laser radiation. The fundamental beam was filtered by using an IR filter. The output from the sample was monochromated to collect 532 nm component and to eliminate the fundamental radiation. The generation of the second harmonic signal was confirmed by the emission of green light. The output SHG voltages for Na-4-HBS and KDP samples were found to be 195 mV and 55 mV respectively. Thus, it was observed that the SHG efficiency of 4HBS crystal was 3.5 times higher than that of KDP.

3.8. Laser damage threshold

Laser-induced damage LID in optical materials refers to permanent damage caused by melting, ablation, cracking, plasma formation etc., when an optical material is exposed to laser radiation. LID threshold refers to the fluence or irradiance which causes such damages. LID threshold of optical materials is getting importance due to high optical intensities involved in nonlinear process and it must withstand high power intensities [23]. A Q-switched Nd:YAG Laser (QUANTA RAY Model LAB-170-10) was used to perform the laser damage threshold test on the grown crystal. The surface LID threshold of Na-4-HBS crystal was calculated using the relation:

$$P(d) = E/\tau A \tag{7}$$

where E is the intensity of the irradiating laser beam [mJ], τ is the pulse width [6 ns] and A is the area of the circular spot size [cm^2]. The calculated LID value of Na-4-HBS is 5.56 GW/cm^2. The subject of material damage is of great importance to the design and successful operation of nonlinear devices and higher value of LDT observed in the grown crystal has proven its usefulness for making laser based devices.

4. Conclusions

Nonlinear optical Na-4-HBS crystal was grown by slow evaporation solution growth technique. The solvent effect on the growth habit was

established. XRD studies revealed crystalline perfection and lattice parameters of the grown crystal. The modes of vibrations of molecules present in Na-4-HBS compound were confirmed by FT-IR spectral analysis. The transmission percentage, lower cutoff wavelength, and optical band gap energy E_g of the grown crystal were examined by UV-Vis spectral analysis. The variation of dielectric constant and dielectric loss was studied as a function of frequency and temperature. The surface laser damage threshold of Na-4-HBS crystal was found to be 5.56 GW/cm^2. The second harmonic generation efficiency of the crystal was found to be 3.5 times higher than that of standard KDP crystal. The higher SHG efficiency, good optical transmission region, low dielectric value and good mechanical strength suggest that the metal organic Na-4-HBS is an efficient NLO material and would be a good alternative for optical, electrical and mechanical devices.

References

[1] JAGANNATHAN K., KALAINATHAN S., GNANASEKARAN T., VIJAYAN N., BHAGAVANNARAYANA G., *Cryst. Res. Technol.,* 42 (2007), 483.

[2] SCHNEIDER A., BIAGGIO I., GUNTER P., *Appl. Phys. Lett.,* 84 (2004), 2229.

[3] JOSE M., SRIDHAR B., BHAGAVANNARAYANA G., SUGANDHI K., UTHRAKUMAR R., JUSTINRAJ C., TAMILVENDHAN D., JEROME DAS S., *J. Cryst. Growth,* 312 (2010), 793.

[4] MUTHU K., MEENAKASHISUNDARAM S.P., *J. Cryst. Growth,* 352 (2012), 158.

[5] GEETHA D., THILAGAVATHI D., *Middle-East J. Sci. Res.,* 4 (3), (2009) 185.

[6] MYTHILI P., KANAGASEKARAN T., SHARMA N.S., GOPALAKRISHNAN R., *J. Cryst. Growth,* 306 (2007), 344.

[7] BRAHADEESWARAN S., VENKATARAMANAN V., SHERWOOD J.N., BHAT H.L., *J. Mater. Chem.,* 8 (3) (1998), 613.

[8] SELVAKUMAR E., ANANDHA BABU G., RAMASAMY P., CHANDRAMOHAN A., *Spectrochim. Acta A,* 122 (2014), 436.

[9] TAFFAREL R.S., RUBIO J., *Miner. Eng.,* 23 (2010), 771.

[10] MOHD. SHAKIR., KUSHWAHA S.K., MAURYA K.K., ARORA M., BHAGAVANNARAYANA G., *J. Cryst. Growth,* 311 (2009), 3871.

[11] ALBERTI G., CONSTANTINO U., ALLULLI S., TOMASSINI N., *J. Inorg. Nucl. Chem.,* 40 (1978), 1113.

[12] KOSNIC E.J., MC CLYMONT E.L., HODDER R.A., SQUATTRITO P.J., *Inorg. Chim. Acta,* 201 (1992), 143.

[13] SILVERSTEIN R.M., WEBSTER F.X., KIEMLE D.J., *Spectrometric Identification of Organic Compounds,* 7th Ed., John Wiley and Sons, New York, 2005.

[14] MARCHEWKA M.K., PIETRASZKO A., *Spectrochim Acta A,* 69 (2008), 312.

[15] ZAHID MD. I., KALAIYARASI S., KRISHNA KUMAR M., GANESH T., JAISANKAR V., MOHAN KUMAR R., *Mater. Sci.-Poland.,* 34 (4) (2016), 81.

[16] KRISHNAKUMAR V., NAGALAKSHMI R., OZGA K., PIASECKI M., KITYK I.V., BRAGIEL P., *J. Optoelectron. Adv. M.,* 11(2) (2009) 123.

[17] RAO C.N.R., *Ultraviolet and Visible Spectroscopy,* 3rd Ed., Butterworths, London, 1975.

[18] ROSHAN A., JOSEPH S.C., *Mater. Lett.,* 49 (2001), 299.

[19] KRISHNAKUMAR V., NAGALAKSHMI R., *Spectrochim. Acta A,* 6 (2005), 499.

[20] RAI R.N., MUDUNURI S.R., REDDI R.S.B., KUMAR SATULURI V.S.A., GANESHMOORTHY S., GUPTA P.K., *J. Cryst. Growth,* 321 (2011), 72.

[21] REICHMAN J., *Handbook of Optical Filters for Fluorescence Microscopy,* Chroma Technology Corp., USA, 1998.

[22] RAO K.V., SMAKULA A., *J. Appl. Phys.,* 36 (6) (1965), 2031.

[23] BHAR G.C., CHAUDHARY A.K., KUMBHAKAR P., *Appl. Surf. Sci.,*161 (2000), 155.

Received 2017-03-14
Accepted 2018-12-18